Supporting Information

From Aluminum Oxo Cluster to Aluminum Oxo Cluster Organic Cage

Yi Zhang,[#] Ran-Qi Chen,[#] San-Tai Wang, Ya-Jie Liu, Wei-Hui Fang,* Jian Zhang

State Key Laboratory of Structural Chemistry, Fujian Institute of Research on the Structure of Matter, Chinese Academy of Sciences, 350002 Fuzhou, P.R. China.

CONTENT

1. Experimental

Materials and general methods

All the reagents and solvents employed were purchased commercially and used as received without further treatment. Aluminum isopropoxide and potassium bromide were acquired from Aladdin Chemical Reagent Shanghai. Aluminum chloride hexahydrate, isopropyl alcohol, acetonitrile, and 1,5-pentanediol were acquired from Sinopharm Chemical Reagent Beijing. pyrazole was acquired from Shanghai Titan Tech. 4-Pyrazolecarboxylic acid was acquired from Bide Pharma Tech.
The Fourier transform infrared spectroscopy (FT-IR) data (KBr pellets) was recorded on a PerkinElmer Spectrum 100 FT-IR spectrometer over a range of 400-4000 cm^{-1}. The energy dispersive spectroscopy (EDS) analyses of single crystals were performed on a JEOL JSM6700F field-emission scanning electron microscope equipped with an Oxford INCA system. The EDS mapping of single crystals after iodine adsorption was performed on a Zeiss Sigma 300 field-emission scanning electron microscope equipped with an OXFORD AZtecOne X-Max^N 20 silicon drift detector. Powder X-ray diffraction (PXRD) data were collected on a Rigaku Mini Flex II diffractometer using CuK radiation (λ = 1.54056 Å) under ambient conditions. The PXRD simulated patterns were obtained using the Mercury. The UV-vis absorbance data were recorded at room temperature using cyclohexane solution as a standard sample on a Perkin Elmer Lamda-365 UV spectrophotometer and scanned at 200-800 nm. The thermogravimetric analyses (TGA) were performed on a Mettler Toledo TGA/SDTA 851e analyzer in a nitrogen atmosphere with a heating rate of 10 ℃/min.The confocal Raman spectrum were recorded on Horiba Jobin Yvon Labram HR Evolution Raman spectrometer at 532 nm.

Synthesis of $[Al_3(py)_3(\mu_3\text{-}O)(HPyzc)_6]\cdot Cl$ (AlOC-96)

A mixture of aluminum chloride hexahydrate (200 mg, 1.32 mmol), 4-Pyrazolecarboxylic acid (250 mg, 2.23 mmol), pyrazole (2 g, 29.38 mmol), and isopropyl alcohol (5 mL) was sealed in a 20 mL vial and transferred to a preheated oven at 100°C for 3 days. When cooled to room temperature, colorless block crystals were obtained. (yield: 52 % based on 4-Pyrazolecarboxylic acid). The crystals are rinsed with ethanol and preserved in a sealed and dry environment. FT-IR (KBr, cm^{-1}): 3455(m), 1622(v), 1564(m), 1460(m), 1340(s), 993(s), 887(s), 792(m).

Synthesis of $[Al_3(py)_3(\mu_3\text{-}O)(HPyzc)_6]\cdot Br$ (AlOC-97)

A mixture of aluminum isopropoxide (200 mg, 0.98 mmol), 4-Pyrazolecarboxylic acid (250 mg, 2.23 mmol), KBr (50mg) and pyrazole (2 g, 29.38 mmol) and isopropyl alcohol (5 mL) was sealed in a 20 mL vial and transferred to a preheated oven at 100°C for 3 days. When cooled to room temperature, colorless block crystals were obtained (yield: 38 % based on $Al(O^iPr)_3$). The crystals are rinsed with isopropyl alcohol and stored in isopropanol solution. FT-IR (KBr, cm^{-1}): 3456(m), 1624(v), 1560(m), 1458(m), 1338(s), 993(s), 887(s), 790(m).

Synthesis of AlOC-98

A mixture of aluminum isopropoxide (200 mg, 0.98 mmol), 4-Pyrazolecarboxylic acid (250 mg, 2.23 mmol), and pyrazole (2 g, 29.38 mmol) and isopropyl alcohol (5 mL) was sealed in a 20 mL vial and transferred to a preheated oven at 100°C for 3 days. When cooled to room temperature, colorless octahedron crystals were obtained (yield: 16 % based on $Al(O^iPr)_3$). The crystals are rinsed with isopropyl alcohol and stored in isopropanol solution. FT-IR (KBr, cm^{-1}): 3310(m), 1680(v), 1542(v), 1480(v), 1420(s), 1315(s), 985(s), 937(m), 800(s).

Optimized Synthesis of AlOC-98

A mixture of aluminum isopropoxide (200 mg, 0.98 mmol), 4-Pyrazolecarboxylic acid (225 mg, 2.23 mmol), pyrazole (2 g, 29.38 mmol), 1,5 pentanediol (1 mL) and acetonitrile (2 mL) was sealed in a 20 mL vial and transferred to a preheated oven at 100 °C for 3 days. When cooled to room temperature, colorless tetrahedron crystals were obtained. (yield: 37 % based on $Al(O^iPr)_3$). The crystals are rinsed with isopropyl alcohol. FT-IR (KBr, cm^{-1}): 3310(m), 1680(v), 1542(v), 1480(v), 1420(s), 1315(s), 985(s), 937(m), 800(s).

General methods for X-ray Crystallography

Crystallographic data of crystal **AlOC-96** was collected on Supernova single crystal diffractometer equipped with graphite-monochromatic Cu-Kα radiation (λ = 1.5418 Å). **AlOC-97, AlOC-98**, **I_2@AlOC-98** were collected on Hybrid Pixel Array detector equipped with Ga-Kα radiation (λ = 1.3405 Å) at 100 K. The structures were solved with the dual-direct methods using ShelXT and refined with the full-matrix least-squares technique based on F^2 using the SHELXL-2014. Non-hydrogen atoms were refined anisotropically. Hydrogen atoms were added theoretically, riding on the concerned atoms, and refined with fixed thermal factors. All absorption corrections were performed using the multiscan program. The diffused electron densities resulting from residual solvent molecules were removed from the data set using the *SQUEEZE* routine of *PLATON* and refined further using the data generated. The 1H-4-pyrazolecarboxylic acid molecules acting as bridges in **AlOC-98**, **I_2@AlOC-98** are distributed statistically. The detailed crystal data for these compounds are given in Table S1.

Iodine/Cyclohexane Adsorption Measurement

The iodine adsorption has been designed and reported previously.[1] Adsorption studies were performed by immersing 60 mg sample in 10 mL of a 1mmol·L^{-1} iodine/cyclohexane solution. The supernatant solution was used for each UV–vis absorbance measurement periodically. After each measurement, the solution was dispensed back into the respective vial to keep the volume constant. The absorbance at the maximum wavelength of iodine (λmax = 521nm) was selected to calculate the iodine content**.** The removal ratios (R) of iodine were calculated using $R = (C_0 - C_t)/C_0 \times 100\%$ (where C_0 and C_t represent the initial concentration and concentration at time t, respectively).

2. Detailed Structure Information and basic characterizations of AlOC-96.

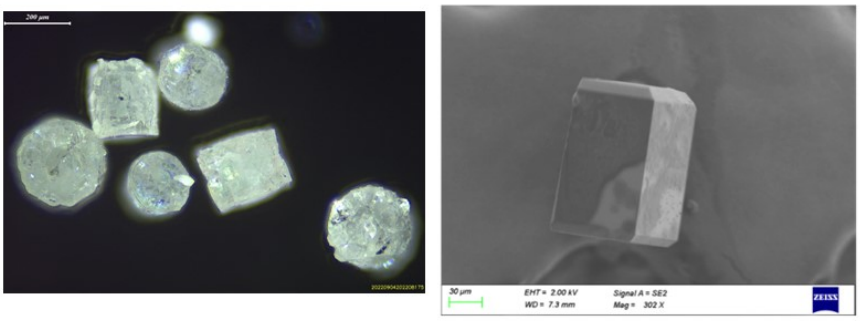

Fig. S1 Microscope image and SEM image **AlOC-96**.

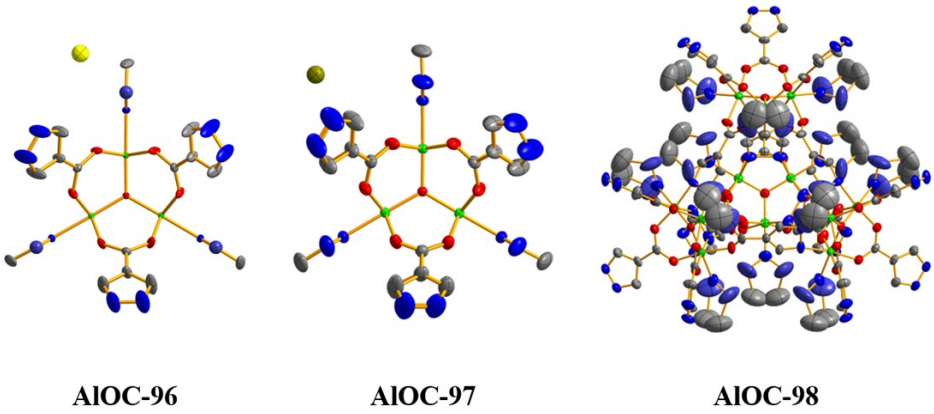

Fig. S2. ORTEP drawing of the compounds. Hydrogen atoms were omitted for clarity. Thermal ellipsoids displayed at 50% probability.

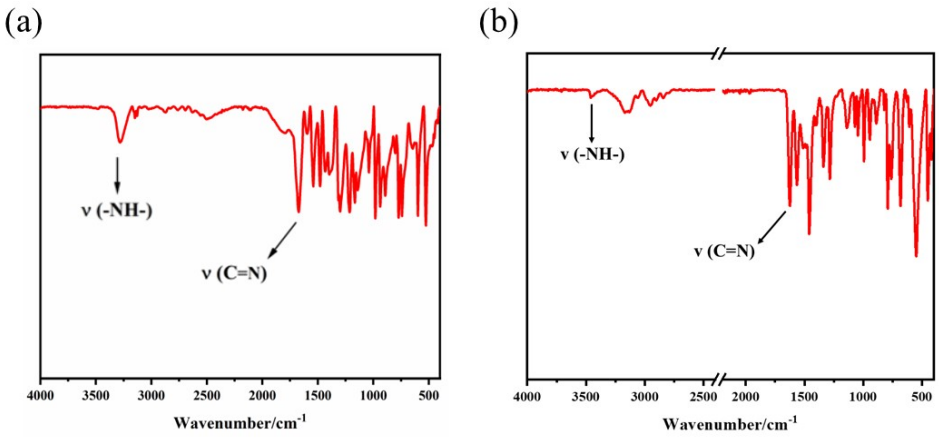

Fig. S3. FT-IR spectrum of (a) 1H-4-pyrazole carboxylic acid and (b) **AlOC-96**.

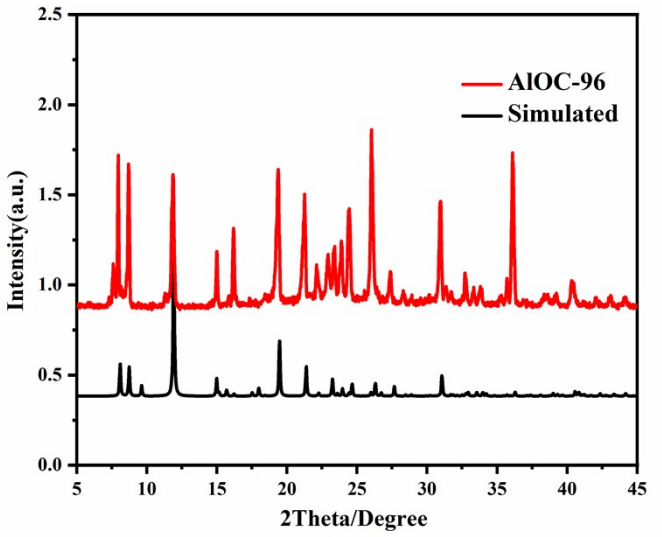

Fig. S4. PXRD pattern of **AlOC-96**.

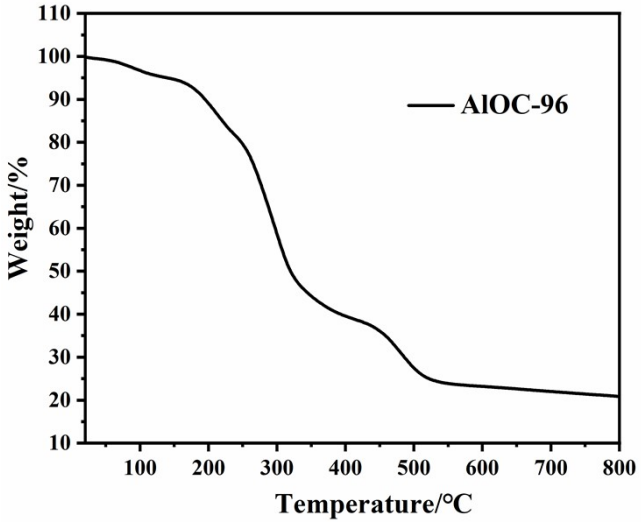

Fig. S5. TGA spectrum of **AlOC-96**.

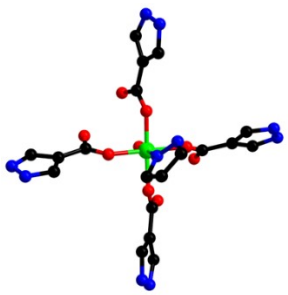

Fig. S6. Coordination mode of each Al^{3+} ion in **AlOC-96**.

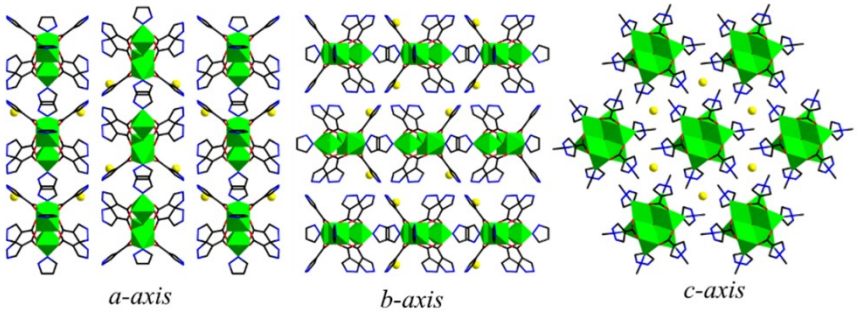

Fig. S7. Packing diagrams of **AlOC-96** in the view of a-axis, b-axis and c-axis.

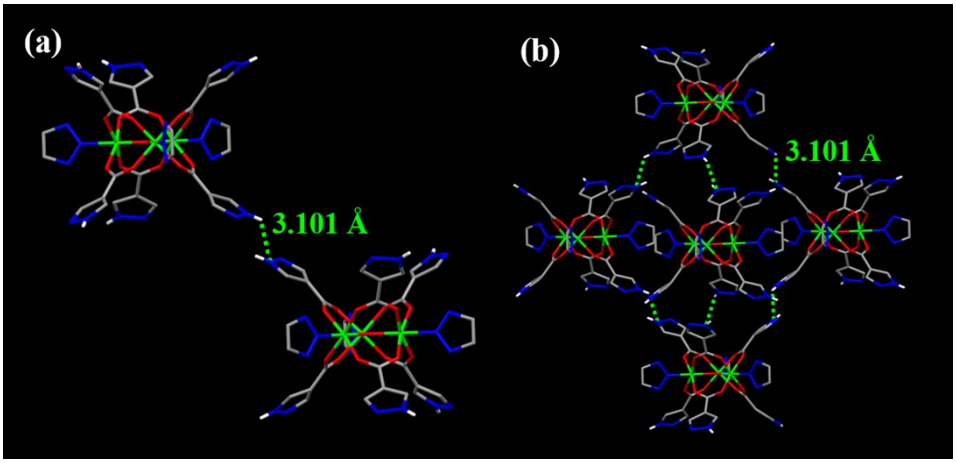

Fig. S8. Hydrogen bond between Al_3 clusters of **AlOC-96.**

3. Detailed Structure Information and basic characterizations of AlOC-97.

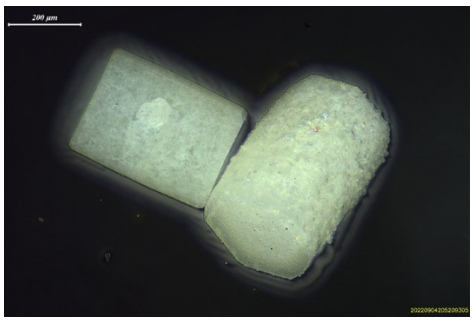

Fig. S9. Microscope image of **AlOC-97**.

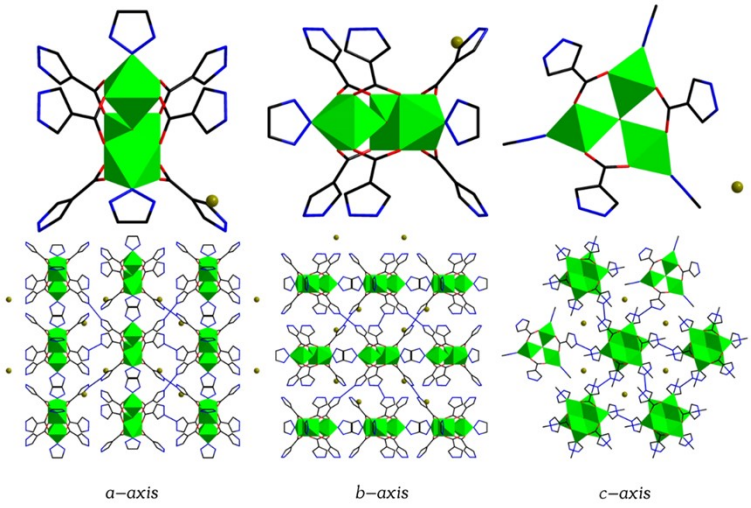

Fig. S10. Crystal views and packing diagrams of **AlOC-97** of a-axis, b-axis, and c-axis.

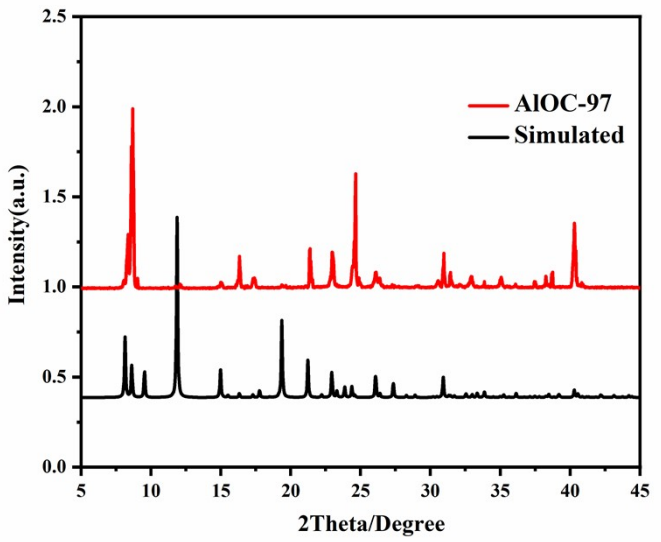

Fig. S11. PXRD pattern of **AlOC-97**.

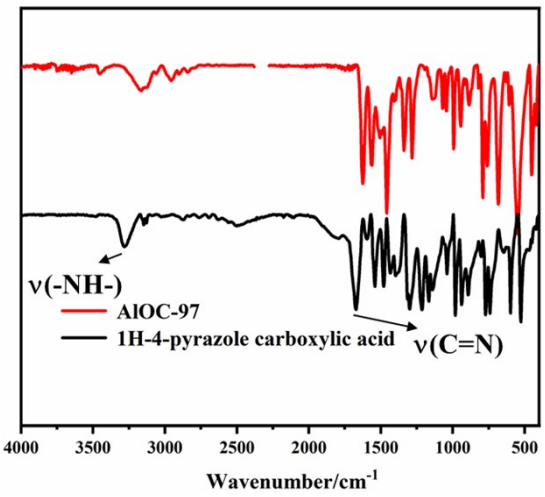

Fig. S12. FT-IR spectrum of **AlOC-97**.

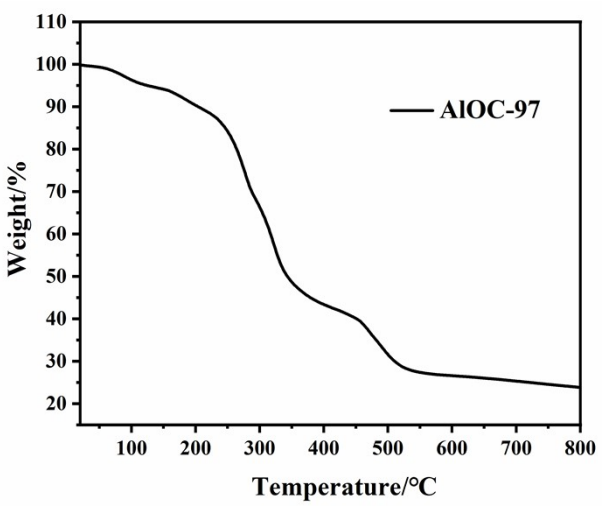

Fig. S13. TGA spectrum of **AlOC-97**.

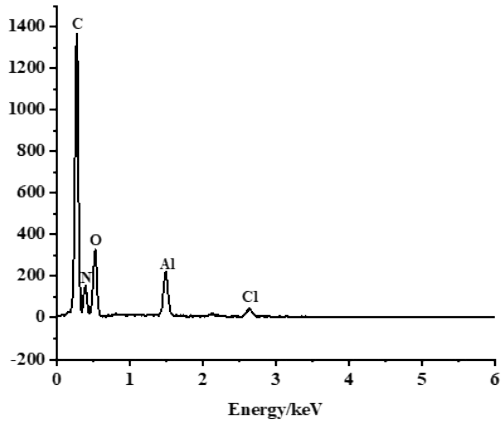

Fig. S14. EDS spectrum of **AlOC-96**.

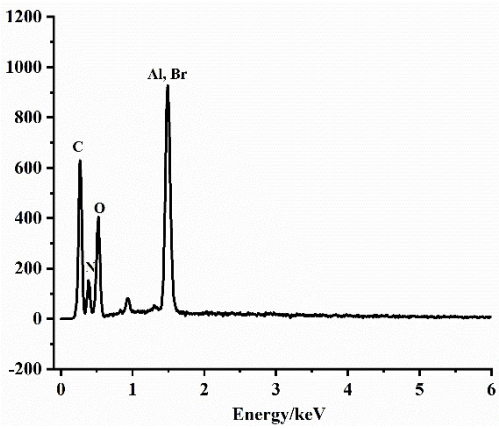

Fig. S15. EDS spectrum of **AlOC-97**.

Detailed Structure Information and basic characterizations of AlOC-98.

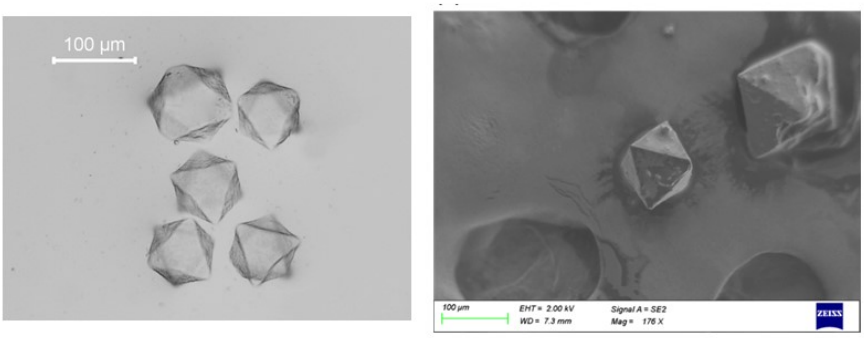

Fig. S16. Microscope image and SEM image of the octahedron of **AlOC-98**.

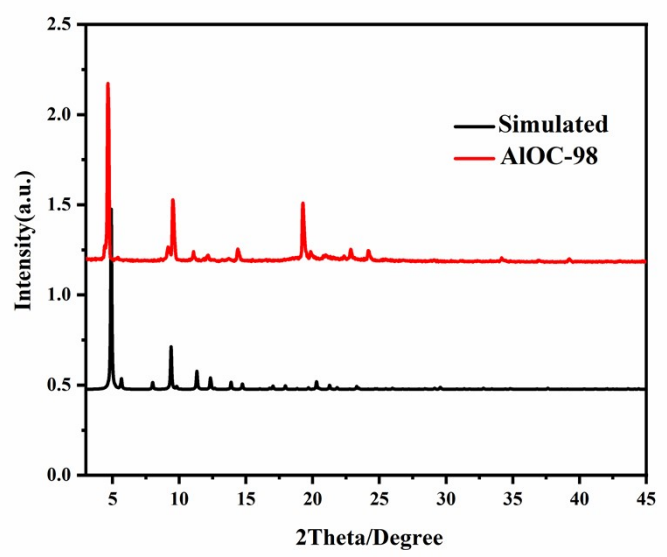

Fig. S17. PXRD pattern of **AlOC-98**.

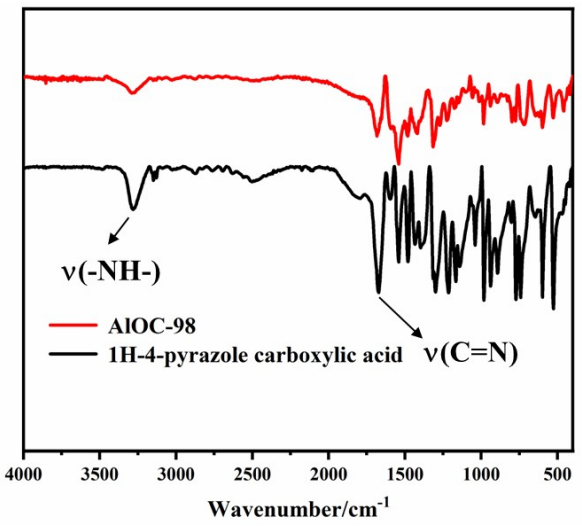

Fig. S18. FT-IR spectrum of **AlOC-98**.

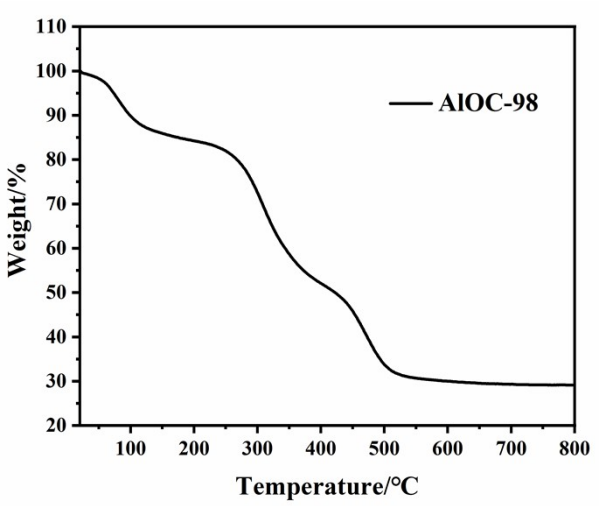

Fig. S19. TGA spectrum of **AlOC-98**.

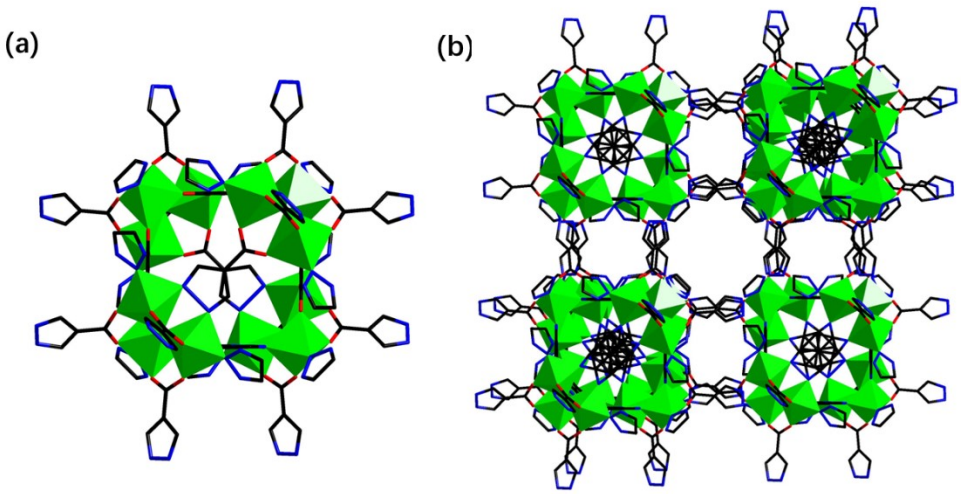

Fig. S20. Crystal views (a) and packing diagrams (b) of **AlOC-98**. (a-axis , b-axis , and c-axis are all the same)

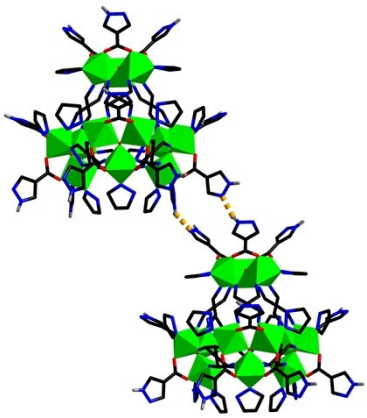

Fig. S21. N-H double hydrogen bond between **AlOC-98**.

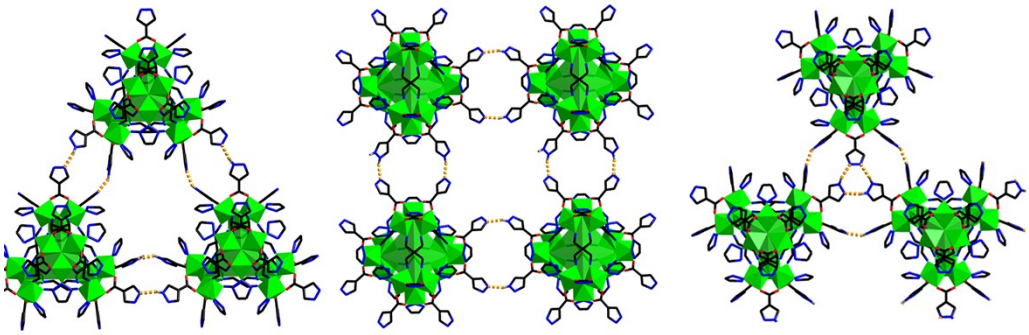

Fig. S22. The hydrogen bonding interactions in **AlOC-98**.

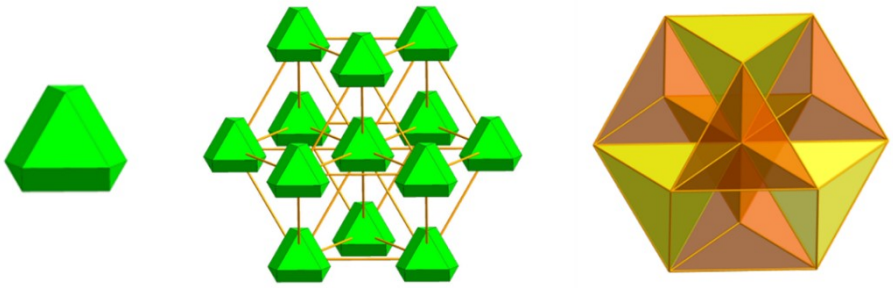

Fig. S23. Topo structure of **AlOC-98** when the tetrahedral as a node, schematic diagram of **Cuboctahedron** topology type of **AlOC-98**.

4. Iodine/Cyclohexane Adsorption Measurement.

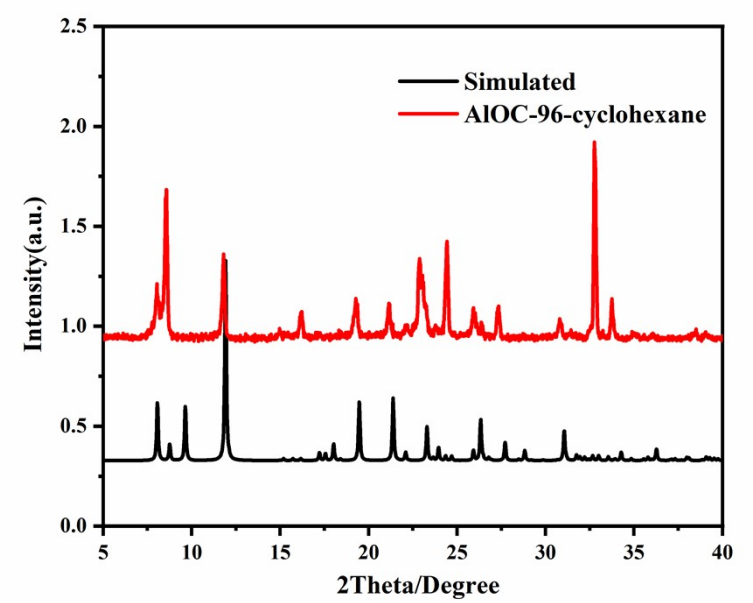

Fig. S24. PXRD pattern of **AlOC-96** after soaking in cyclohexane for 24 h.

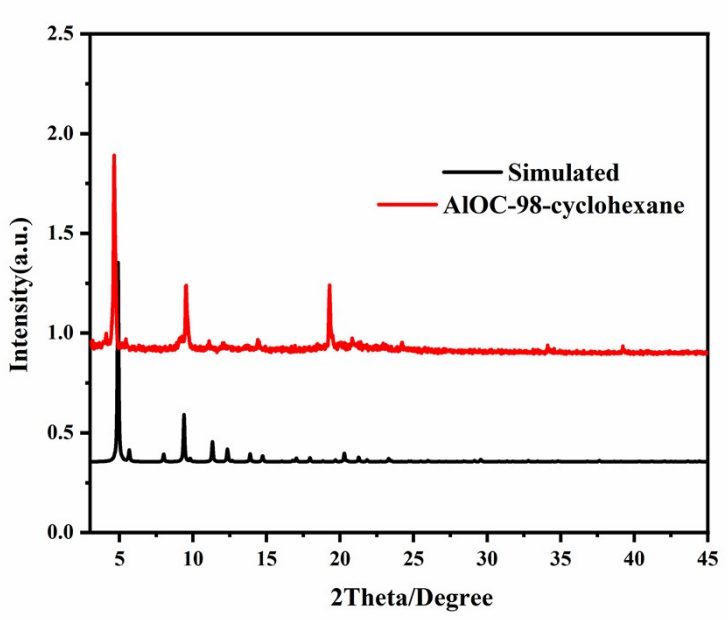

Fig. S25. PXRD pattern of **AlOC-98** after soaking in cyclohexane for 24 h.

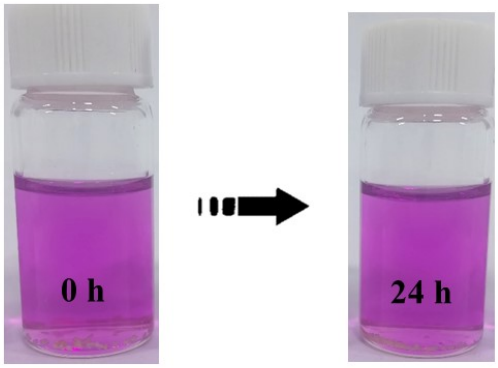

Fig. S26. The color of 1mmol·L^{-1}Iodine/cyclohexane is no change in color when single crystals of **AlOC-96** were immersed within 24 hours.

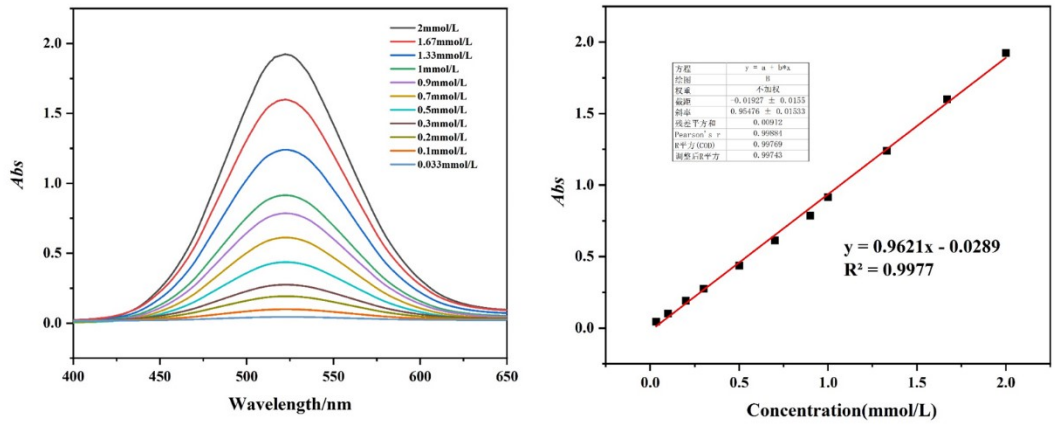

Fig. S27. Calibration plots of standard iodine by UV-vis spectrum in cyclohexane solution.

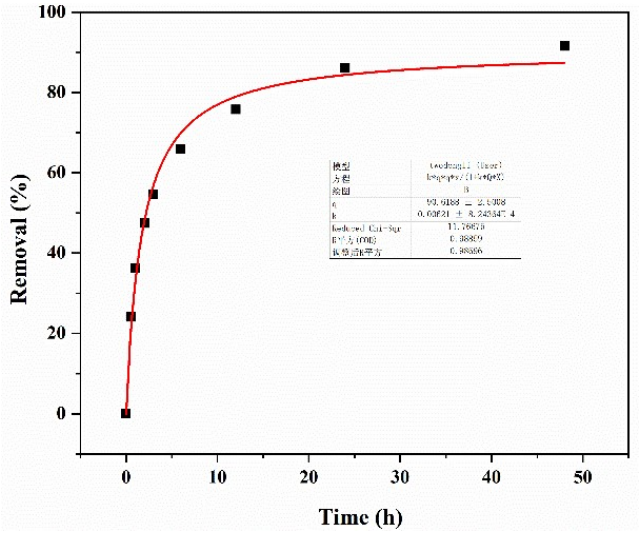

Fig. S28. Iodine adsorption kinetics of **AlOC-98**.

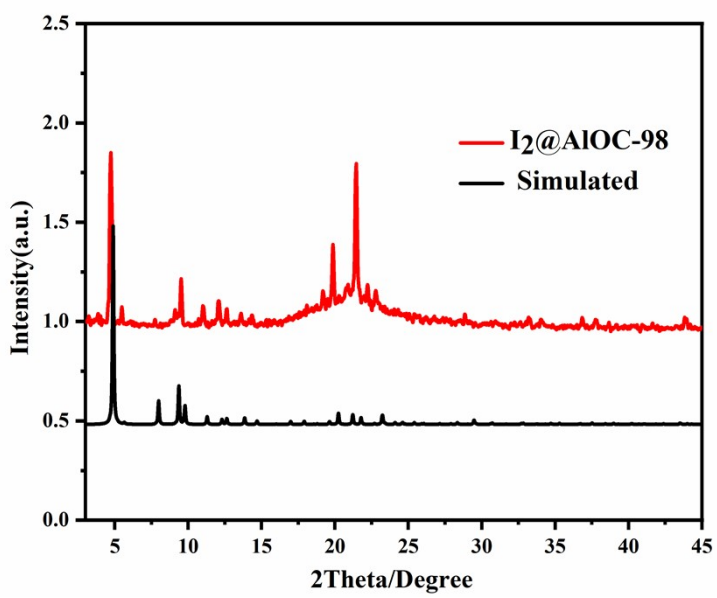

Fig. S29. PXRD patterns of **I_2@AlOC-98**.

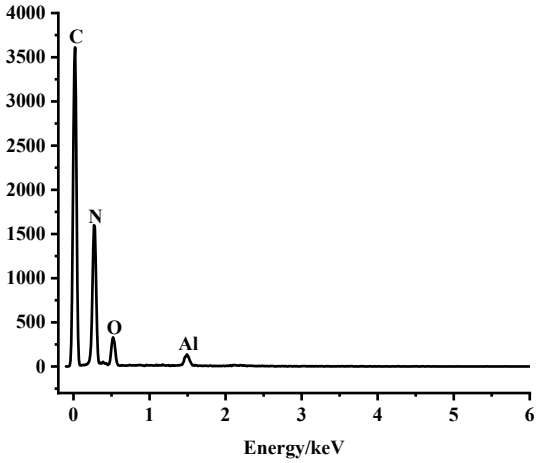

Fig. S30. EDS spectrum of **AlOC-98**.

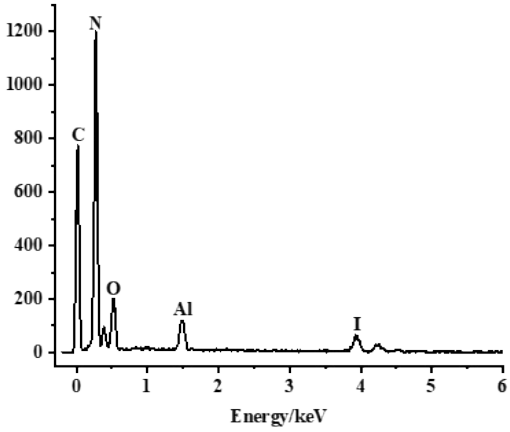

Fig. S31. EDS spectrum of **I_2@AlOC-98**.

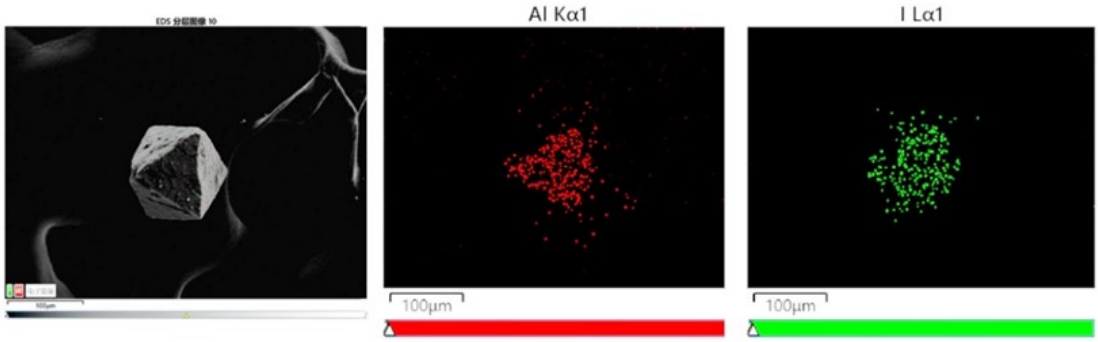

Fig. S32. EDS-mapping spectrum of **I_2@AlOC-98**. From left to right are crystal appearance, aluminum, and iodine elements.

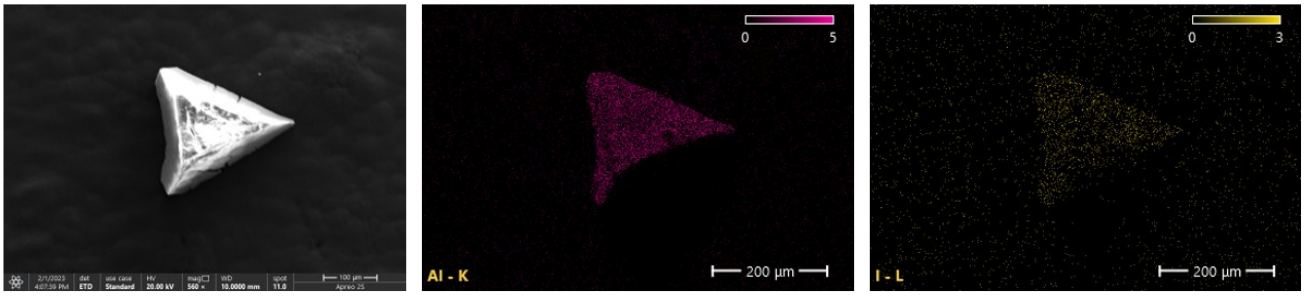

Fig. S33. EDS-mapping spectrum of the transverse section of the **I_2@AlOC-98**. From left to right are crystal appearance, aluminum, and iodine elements.

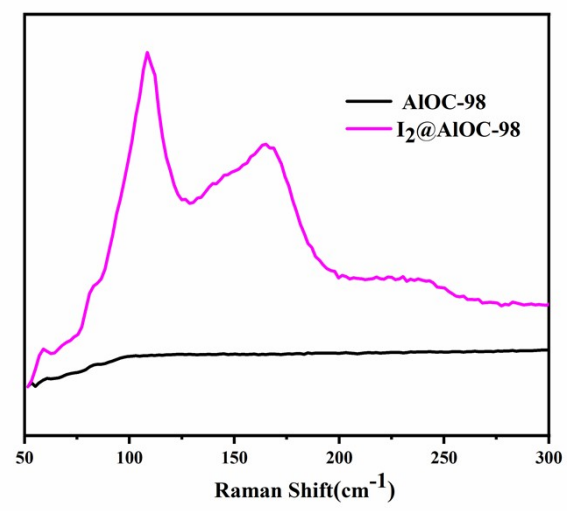

Fig. S34. Comparison Raman spectrum of **AlOC-98** and **I_2@AlOC-98** in the low energy region. (**I_2@AlOC-98** were obtained by soaking fresh samples in iodine/cyclohexane solutions (10 mL, 1mmol·L−1) for 24 hours).

Raman spectrum confirmed the existence of iodine species in **I_2@AlOC-98**. The new peak appeared at ~108, 165 cm^{-1} for **I_2@AlOC-98**.

5. Supporting Tables

Table S1. Crystal data and structure refinement results (**AlOC-96**, **AlOC-97, AlOC-98, and I_2@ AlOC-98**).

Compound	AlOC-96	AlOC-97	AlOC-98	I_2@AlOC-98
Formula	$C_{39}H_{48}Al_3ClN_{18}O_{16}$	$C_{39}H_{46}Al_3BrN_{18}O_{15}$	$C_{242}H_{452}Al_{12}N_{60}O_{86}$	$C_{108}H_{96}Al_{12}N_{60}O_{40}$
*M*r	1125.32	1167.76	5901.94	3293.94
Temperature(K)	100.15	100.02	100.15	99.99
Wavelength (Å)	1.54184	1.34050	1.34050	1.34050
Crystal system	hexagonal	hexagonal	cubic	cubic
Space group	*P6$_3$/m*	*P6$_3$/m*	*F-4$_3$m*	*F-4$_3$m*
a/Å	11.6805(6)	11.8356(5)	31.2358(2)	31.3195(4)
b/Å	11.6805(6)	11.8356(5)	31.2358(2)	31.3195(4)
c/Å	21.8391(12)	21.7059(10)	31.2358(2)	31.3195(4)
α/°	90	90	90	90
β/°	90	90	90	90
γ/°	120	120	90	90
V/Å^3	2580.4(3)	2633.2(2)	30476.0(6)	30721.6(12)
Z	2	2	4	4
ρ/g cm^{-3}	1.448	1.473	1.286	0.712
μ/mm^{-1}	1.869	1.491	0.718	0.507
F(000)	1168.0	1200.0	12680.0	6752.0
Collected reflns	10533	11191	9229	20891
Unique reflns (R_{int})	1831(0.0544)	2063(0.0396)	2993(0.0145)	2854(0.0452)
Completeness	1	1	0.92	0.9883
GOF on F^2	1.155	1.090	1.079	1.080
R_1[a]/wR_2[b][$I > 2(I)$]	0.0483/0.1445	0.0522 / 0.1497	0.0442/0.1221	0.0531/0.1582

[a] $R_1 = \Sigma||F_o|-|F_c||/\Sigma|F_o|$ [b] $wR_2 = \{\Sigma[w(F_o^2-F_c^2)^2]/\Sigma[w(F_o^2)^2]\}^{1/2}$

Table S2 Bond valence sum (BVS) analysis for Al and μ_3-O of **AlOC-96**, **AlOC-97**, **AlOC-98**

AlOC-96	
Al01 3.1294 Al01—O003 1.822(5) 0.629 Al01—O004[1] 1.911(6) 0.494 Al01—O004[2] 1.911(6) 0.494 Al01—O005 1.905(3) 0.503 Al01—O005[3] 1.905(3) 0.503 Al01—N006 2.042(3) 0.506	O003 1.8872 O003—Al1 1.822(5) 0.629 O003—Al1[2] 1.822(5) 0.629 O003—Al1[4] 1.822(5) 0.629
Symmetry code: [1]-y,+x-y,+z; [2]-y,+x-y,1/2-z; [3]+x,+y,1/2-z; [4]+y-x,-x,1/2-z; Bond valence = exp((Ro-R)/B), where Ro values for Al-O bond length and Al-N bond length are 1.651 and 1.79 respectively, B is 0.37.	
AlOC-97	
Al01 3.1445 Al01—O003 1.825(7) 0.624 Al01—O004[1] 1.905(3) 0.503 Al01—O004[2] 1.905(3) 0.503 Al01—O005 1.896(3) 0.515 Al01—O005[3] 1.896(3) 0.515 Al01—N006 2.058(2) 0.484	O003 1.8710 O003—Al01 1.825(7) 0.624 O003—Al01[2] 1.825(7) 0.624 O003—Al01[4] 1.825(7) 0.624
Symmetry code: [1]2-Y,1+X-Y,3/2-Z; [2]2-Y,1+X-Y,+Z; [3]+X,+Y,3/2-Z; [4]1+Y-X,2-X,3/2-Z; Bond valence = exp((Ro-R)/B), where Ro values for Al-O bond length and Al-N bond length are 1.651 and 1.79 respectively, B is 0.37.	
AlOC-98	
Al01 3.427 Al01—O02 1.813(8) 0.644 Al01—O03[1] 1.913(7) 0.492 Al01—O03 1.913(7) 0.492 Al01—N005 2.000(3) 0.566 Al01—N008 1.968(8) 0.617 Al01—N008 1.968(8) 0.617	O02 1.932 O02—Al01 1.812(9) 0.644 O02—Al01[2] 1.812(9) 0.644 O02—Al01[3] 1.812(9) 0.644
Symmetry code: [1]+X,+Z,+Y; [2]1-Y, 1-X,+Z; [3]1-Y, +Z , 1-X; Bond valence = exp((Ro-R)/B), where Ro values for Al-O bond length and Al-N bond length are 1.651 and 1.79 respectively, B is 0.37.	

Table S3. Kinetic parameters of the pseudo-second-order model for iodine adsorption toward **AlOC-98** (1mmol/L).

Sample	C_0 (mmol·L^{-1})	Removal (%)	Second-order kinetic model			
			q_e (mg·kg^{-1})	h (mg·kg^{-1})	k (mg·kg^{-1}·h^{-1})	R_2
AlOC-98	1mmol·L^{-1}	91.5	93.120	53.724	0.00621	0.987

Sorption kinetics of iodine in **AlOC-98** was fitted to a pseudo-second-order kinetics model, $t/q_t = 1/h + t/q_e$ (where q_t, q_e represent the amounts of adsorbate at certain time t or at equilibrium time, h is the initial adsorption rate, $h = kqe^2$, and k is the rate constant).

6. Reference

1. C.-H. Liu, W.-H. Fang, Y. Sun, S. Yao, S.-T. Wang, D. Lu and J. Zhang, *Angew. Chem. Int. Ed.*, 2021, **60**, 21426-21433.